Rare Metal Materials and Engineering
Volume 53, Issue 9, September 2024
Available online at www.rmme.ac.cn

Science Press

Cite this article as: Lao Zhenhong, Zhang Haoyu, Wang Shengyuan, et al. Effect of Different Sizes of *α* Phase on Tensile Properties of Metastable *β* Titanium Alloy Ti-5.5Cr-5Al-4Mo-3Nb-2Zr[J]. Rare Metal Materials and Engineering, 2024, 53(09): 2430-2437. DOI: 10.12442/j.issn.1002-185X.20230791.

ARTICLE

Effect of Different Sizes of *α* Phase on Tensile Properties of Metastable *β* Titanium Alloy Ti-5.5Cr-5Al-4Mo-3Nb-2Zr

Lao Zhenhong[1], Zhang Haoyu[1], Wang Shengyuan[1], Cheng Jun[2], Tan Bing[1], Zhou Ge[1], Zhang Siqian[1], Chen Lijia[1]

[1] School of Materials Science and Engineering, Shenyang University of Technology, Shenyang 110870, China; [2] Shaanxi Key Laboratory of Biomedical Metal Materials, Northwest Institute for Nonferrous Metal Research, Xi'an 710016, China

Abstract: To study the relationship between the microstructure and tensile properties of the novel metastable *β* titanium alloy Ti-5.5Cr-5Al-4Mo-3Nb-2Zr, a heat treatment process of ABFCA (solid solution in *α*+*β* region with subsequent furnace cooling followed by aging treatment finally) was designed, by which *α* phases of different sizes can be precipitated in the *β* matrix. The results show that the microstructure obtained by this heat treatment process is composed of primary *α* (α_p) phase, submicro rod-like *α* (α_r) phase and secondary *α* (α_s) phase. The alloy with multi-scale *α* phase has an excellent balance between strength and ductility. The elongation is about 18.3% at the ultimate tensile strength of 1125.4 MPa. The relationship between the strength of the alloy and the *α* phase was established. The strength of the alloy is proportional to the power of −1/2 of the average spacing and width of *α* phase. The α_s phase with a smaller size and phase spacing can greatly improve the strength of the alloy by hindering dislocation slip. The transmission electron microscope analysis shows that there is a large amount of dislocation accumulation at the *α*/*β* interfaces, and many deformation twins are found in the α_p phase after tensile deformation. When the dislocation slip is hindered, twins occur at the stress concentration location, and twins can initiate some dislocations that are difficult to slip. Meanwhile, the plastic strain is distributed uniformly among the α_p, α_r, α_s phases and *β* matrix, thereby enhancing the ductility of the alloy.

Key words: metastable *β* titanium alloy; *α* phase; heat treatment; tensile properties

According to previous studies, the importance of metastable *β* titanium alloys is gradually increasing, and this type of alloy can obtain high strength after strengthening[1]. For instance, the ultimate tensile strength (UTS) of Ti-13V-3Al-11Cr (wt%) alloy can reach up to 1350 MPa[2], and Ti55531 (Ti-5Al-5V-5Mo-3Cr-1Zr) alloy possesses an extremely high strength above 1400 MPa after heat treatment[3]. Furthermore, after aging treatment, the UTS of Ti-3Al-4Zr-4Mo-8V-6Cr metastable *β* titanium alloy can even reach an impressive value (about 1624 MPa)[4]. In addition, metastable *β* titanium alloy has the advantages of lightweight and outstanding corrosion resistance and fatigue properties, so metastable *β* titanium alloy has been widely used in advanced engineering fields such as aerospace, automotive and other fields[5]. The Ti-15V-3Cr-3Al-3Sn alloy has been used to make cold-formed sheets and springs for aircraft[6]. Ref.[7] mainly introduced the high strength metastable *β* titanium alloy Ti-1300, which was developed independently in China, and parts made of this alloy have been used in some Chinese aircraft engines. Ti-8V-6Cr-4Mo-3A1-4Zr (Ti-86434) alloy is used in automotive fasteners[8]. However, it is a challenge to achieve high strength and good ductility due to the inherent trade-off between the two properties during heat treatment processes. For example, solution treatment plays a crucial role in the heat treatment of metastable *β* titanium alloys. Solution treatment at temperatures above and below the phase transformation temperature (T_β) was performed, followed by aging treatment. The lamellar microstructure (LM) and bimodal microstructure (BM) of the Ti600 alloy can be obtained. Alloy with LM shows high UTS (1300 MPa), but an extremely poor elongation (EL) of 3.2% is obtained. However, the alloy with BM possesses a comparatively outstanding EL (15%), and the

Received date: December 06, 2023
Foundation item: National Natural Science Foundation of China (52104379, U21A20117, 52071219, 52271249)
Corresponding author: Zhang Haoyu, Ph, D., Professor, School of Materials Science and Engineering, Shenyang University of Technology, Shenyang 110870, P. R. China, E-mail: zhanghaoyu@sut.edu.cn

UTS decreases by nearly 300 MPa[9]. Zhang et al[10] designed a novel Ti-6Mo-5V-3Al-2Fe alloy (wt%). After aging treatment at 500 °C/8 h, the α_s phase with a width less than 100 nm is precipitated, and an extremely high UTS (1500 MPa) and poor EL (5%) are obtained. However, by adjusting the size, distribution and volume fraction of the α_s phase, the EL of the alloy can be increased to 12%, but the strength is reduced to less than 1200 MPa. Therefore, a conclusion can be made that the tensile properties are affected by the distribution, volume fraction, size and morphology of the α phase[11]. These characteristics of the α phase can be changed by heat treatment processes. Therefore, extensive research has been carried out to regulate the microstructure of metastable β titanium alloys by heat treatment and to optimize the delicate balance between strength and ductility[12–14].

The metastable β titanium alloy Ti-3.5Al-5Mo-6 V-3Cr-2Sn was aged at 440 °C for 6 h, and the α_s phase with a width of 50 nm, spacing of 85 nm and volume fraction of 61% was obtained. Meanwhile, an extremely high UTS of 1613 MPa and an acceptable EL of 8.3% are obtained[15]. Dong et al[16] investigated the Ti-7333 alloy. This alloy composed of α_p phase (30vol%) and α_s phase with 30 nm in width exhibits the best tensile properties (UTS=968 MPa and EL=13.9%). The multi-sized α phase in Ti-55531 alloy was found[17]. The specimens achieve a superior balance between strength and ductility through a two-stage aging treatment process, with UTS=1120 MPa and EL=19.5% obtained from the tensile test. The impact of solution treatment and aging treatment processes on the microstructure and tensile properties of Ti-55531 alloy was investigated by Chen et al[18]. Song et al[19] studied the formation of intermediate phases and their influences on the microstructure of high strength titanium alloy. The yield strength of Ti-5321 alloy heated at slow or fast rate is comparable due to similar intragranular α precipitate features. However, in comparison with α layers with continuous grain boundary developed in rapidly heated sample, the slowly heated sample with discontinuous grain boundary α colonies has better ductility. Yuan et al[20] studied the microstructure and mechanical properties of self-designed metastable β titanium alloy Ti-7.46V-5Mo-3.13Cr-1Zr-3Al. Based on the comprehensive comparison of the experimental results, it can be determined that the alloy can achieve a good match of strength and plasticity after triple cold rolling annealing at 800 °C/20 min and aging at 500 °C/10 h, the tensile strength is 1380 MPa and the EL is 10.8%.

The size and morphology of the α_s phase are determined by the aging temperature and time. The optimal heat treatment parameters for the Ti-55531 alloy are determined as follows: solution treatment at 880 °C for 1.5 h, followed by aging treatment at 620 °C for 10 h. Song et al[21] studied the effect of heat treatment on the microstructures and mechanical properties of Ti-5Fe-3V-2Cr-2Al (Ti-5322) alloy. Compared with the samples annealed in the β region and subsequently aged, the samples annealed in the α/β region and then aged (800 °C for 1 h and 550 °C for 6 h) exhibit superior ductility attributed to the presence of the α_p phase. The results show that the α_p and α_s phases of metastable β titanium alloy are significantly affected by heat treatment processes, and the strength and ductility of the alloy are greatly changed.

The relationship between α phases and tensile properties after heat treatment of the Ti-5.5Cr-5Al-4Mo-3Nb-2Zr alloy, a novel metastable β titanium alloy, remains unclear. For this reason, the microstructure of the alloy was modulated by various heat treatment procedures, and subsequently, the α phase was characterized by scanning electron microscope (SEM), X-ray diffraction (XRD) and transmission electron microscope (TEM) with selected-area electron diffraction (SAED). The tensile test was employed to evaluate the strength and ductility of the alloy. The impact of the α phase on the strength and ductility of the alloy was investigated. The aim is to provide a reference for formulating the heat treatment process of Ti-5.5Cr-5Al-4Mo-3Nb-2Zr alloy and to establish a theoretical foundation for regulating the microstructure and properties of metastable β titanium alloys.

1 Experiment

The composition of the Ti-5.5Cr-5Al-4Mo-3Nb-2Zr (wt%) alloy was designed based on d-electron theory and Mo equivalent ($[Mo]_{eq}$)[22], and the formulas are as follows:

$$\overline{Bo} = \sum_{n=1}^{k} X_n (Bo)_n \tag{1}$$

$$\overline{Md} = \sum_{n=1}^{k} X_n (Md)_n \tag{2}$$

$$[Mo]_{eq} = [Mo] + 0.28[Nb] + 0.67[V] + 1.25[Ni] + 1.7[Mn] + 2.5[Fe] \tag{3}$$

where X_n refers to the atomic fraction of element n; $(Bo)_n$ and $(Md)_n$ represent the values of the n component. The Bo value is calculated to be 2.77, the Md value is determined as 2.37, and the Mo equivalent value is measured to be 14.64. The alloy is composed of sponge Ti, 70%-purity Nb-Al alloy, and 80%-purity Mo-Al alloy, as well as pure Cr and Zr. The raw materials were melted by vacuum arc melting, and then the molten alloy was cast and forged. The actual composition of the metastable β titanium alloy Ti-5.5Cr-5Al-4Mo-3Nb-2Zr was obtained by gas analysis (Table 1). The T_β of the alloy was measured to be 835 °C, which was measured by calculation and metallographic methods.

The heat treatment process setting, including aging treatment (600 °C/6 h, air cooling (AC)) named as SX, solution treatment (800 °C/0.5 h, water cooling (WC)) named as

Table 1 Chemical composition of Ti-5.5Cr-5Al-4Mo-3Nb-2Zr (wt%)

Cr	Al	Mo	Nb	Zr	Fe	O	Ti
5.41	4.98	4.10	3.12	2.16	0.03	0.08	Bal.

GR, and ABFCA treatment (800 °C/0.5 h solution treatment followed by furnace cooling (FC) and aging treated finally at 600 °C for 6 h with AC, Fig. 1) is presented in Table 2. ABFCA heat treatment process can not only obtain α_p, α_s and α_r, but also avoid energy waste and thus save time and cost.

The samples were sealed in a quartz tube filled with argon gas atmosphere, and three samples were tested for each set of experiments.

A tensile samples with a gauge length of 20 cm was cut from the forged plate parallel to the rolling direction. Three samples were tested to obtain an average value. The tensile tests were conducted on the MTS Landmark 370.10 testing machine at a constant speed of 0.5 mm/min, and tensile experimental data such as UTS, yield strength (YS) and EL can be obtained. After the tensile test, the fracture morphology was performed on an SU-8000 SEM.

After heat treatment, the sample was initially subjected to sanding, followed by mechanical and chemical polishing processes, until a bright surface was obtained. The obtained sample was etched by Kroll's solution (5.5vol% HF+4.5vol% HNO_3+90vol% H_2O). Microstructural characterization was performed on an SU-8010 SEM.

The sample with 400 μm in thickness was cut from the heat-treated sample, thinned to 50 μm and double-jet electropolished in a solution (5vol% $HClO_4$+36vol% $C_4H_{10}O$+59vol% CH_4O) at −20 °C. Microstructure observation was performed on a JEM-2100 TEM.

2 Results and Discussion

2.1 SEM microstructure investigation

The microstructure of the forged alloy is depicted in Fig. 2a. The alloy consists of a single phase, which has been confirmed as the β phase through XRD analysis (Fig.2b). The structure is homogeneous, and the grains remain equiaxed.

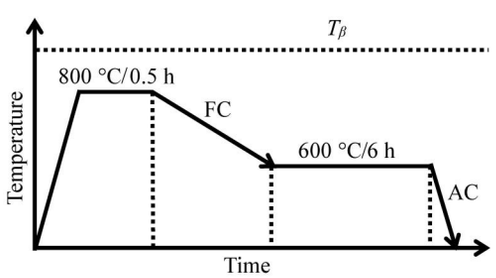

Fig.1 Schematic of ABFCA heat treatment process of Ti-5.5Cr-5Al-4Mo-3Nb-2Zr alloy

Table 2 Parameter setting of different heat treatments

Heat treatment	Solution treatment	Aging treatment
SX	/	600 °C/6 h, AC
ABFCA	800 °C/0.5 h, FC	600 °C/6 h, AC
GR	800 °C/0.5 h, WC	/

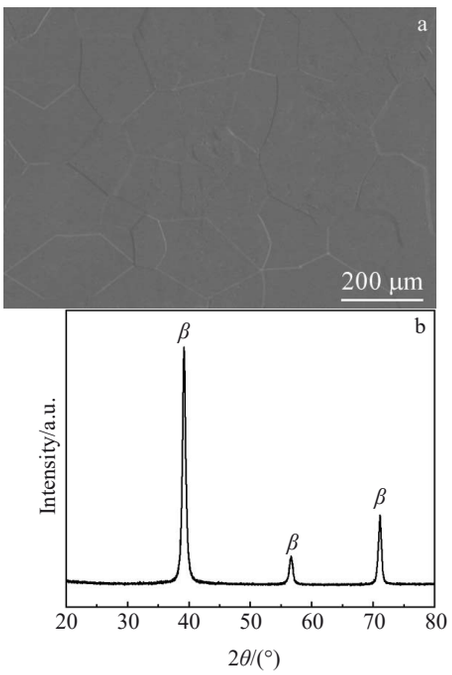

Fig.2 SEM image (a) and XRD pattern (b) of forged alloy

Fig. 3a, 3c and 3e display SEM images of microstructure of the heat-treated sample, and microstructure was processed by MIAGE J software (Fig. 3b, 3d and 3f). Fig. 3a and 3b show the microstructure of the alloy after aging treatment. The ω phase does not form during the phase transition process, the metastable β phase can be directly transformed into the α_s phase, and the α_s phase is directly formed on the dislocation and grain boundary. The transformation driving force plays a dominant role in the precipitation of the α_s phase in the Ti-5.5Cr-5Al-4Mo-3Nb-2Zr alloy[23]. When the temperature is 600 °C, the transformation driving force is larger, so a large number of fine α_s phases can be precipitated. The α_s phase of the alloy was quantitatively analyzed, and the content of the α_s phase is 25.3vol%, the phase spacing is 205 nm, and the aspect ratio of the α_s phase is 11.2. The phase transformation kinetics of aging treatments obviously affects the precipitation behavior of α phase and the mechanical properties of the alloy as well[24].

The tensile properties of the alloy are determined by the grain size[25], which is influenced by the solution temperature. The α_p phase is preferentially accumulated at the grain boundaries, thereby inhibiting grain growth, and the obtained grains are finer. The presence of the α_p phase can improve the ductility of the alloy. The α_p phase is obtained after solution treatment (800 °C/0.5 h) below the T_β of the alloy. The SEM image in Fig.3c clearly shows the morphology of the α_p phase. The α_p phase exhibits an average width of 1.35 μm and an aspect ratio of 2.5, and the content of the α_p phase is 13.5vol% (Fig.3d).

The microstructure of the alloy after ABFCA treatment is shown in Fig. 3e. When the α phase in the alloy begins to

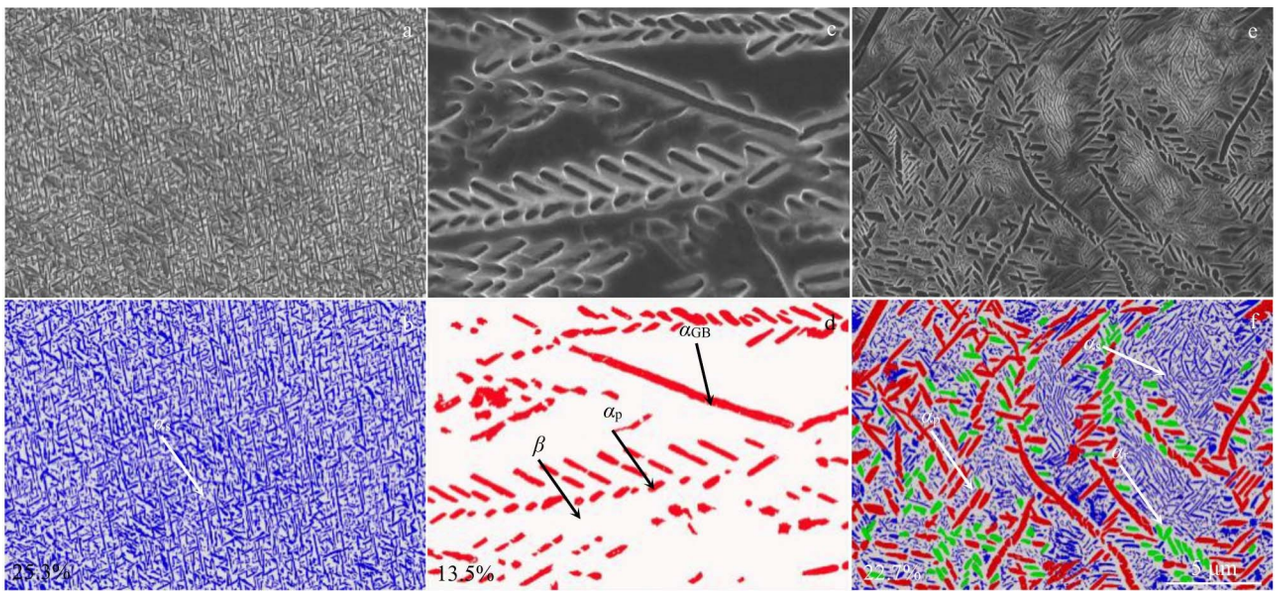

Fig.3 SEM images (a, c, e) and quantitative image analyses (b, d, f) of microstructures of Ti-5.5Cr-5Al-4Mo-3Nb-2Zr alloy after different heat treatments: (a–b) SX, (c–d) GR, and (e–f) ABFCA (red color representing α_p, blue color representing α_s precipitates and green color representing α_r precipitates; the value in the lower left corner of Fig.3b, 3d, and 3f is the volume fraction of α phase)

precipitate, the initial α_p phase (α phase obtained by solution treatment) forms a large precipitate with prolonging the holding time. The nucleation and growth of α_r phase (α phase nucleated during the subsequent cooling process at intermediate temperature) are late, so a medium-sized precipitated phase can be obtained, and the α_s phase (α phase nucleated during the low-temperature aging process) is the smallest α phase. Intragranular precipitates exhibit various morphologies, including the α_p, α_s and α_r phases, all of which are distributed homogeneously within the β matrix. The α_p phase has a width of 1.05 μm and an aspect ratio of 1.5 in average, the α_s phase has an average width of 407 nm and the average length of 2 μm, and the α_r phase has an average length of 0.85 μm and a width of 0.23 μm.

2.2 Room temperature tensile properties

Engineering stress-engineering strain curves of the alloy are obtained by tensile testing at room temperature (Fig.4). When the Ti-5.5Cr-5Al-4Mo-3Nb-2Zr alloy is aged at 600 °C for 6 h, the alloy exhibits an exceptional UTS of 1224.3 MPa, while its EL is significantly limited to merely 5.2%. Compared with the alloy after aging treatment, the strength of the alloy after solution treatment (800 °C/0.5 h) is decreased, but the ductility is obviously improved. Low strength (UTS= 886.9 MPa) and excellent ductility (EL=19.2%) are measured. After ABFCA treatment, the strength and ductility of the alloy reach a very high level, with UTS=1125.4 MPa and EL= 18.3%. A superior combination of strength and ductility is achieved.

The crystal structure of the α phase is hexagonal close-packed, and that of the β phase is face-centered cubic[26], so the slip system of the β phase is more than that of the α phase. Lattice mismatches can occur at the α/β interface, making it difficult for dislocations to slip. The higher the

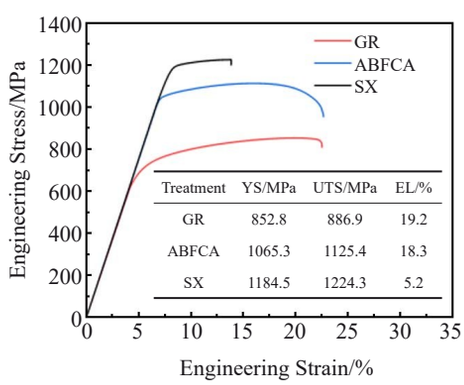

Treatment	YS/MPa	UTS/MPa	EL/%
GR	852.8	886.9	19.2
ABFCA	1065.3	1125.4	18.3
SX	1184.5	1224.3	5.2

Fig.4 Engineering stress-engineering strain curves of Ti-5.5Cr-5Al-4Mo-3Nb-2Zr under different heat treatments (inset table describes the related tensile properties)

volume fraction of the α phase, the more the α/β interfaces to be obtained, thereby enhancing the strength of the alloy.

2.3 Fractography

Fig. 5 presents the fracture surfaces of the Ti-5.5Cr-5Al-4Mo-3Nb-2Zr alloy after heat treatments. Fig. 5a shows the fracture morphology of the samples after aging treatment. The fracture mode of the sample is typical intergranular fracture, and a large number of cleavage surfaces, secondary cracks and a small number of dimples can be observed on the surface. When this brittle fracture characteristic appears on the surface of the fracture, the alloy has a very low ductility, which is confirmed by the tensile curve. The fracture morphology after solution treatment is displayed (Fig. 5b). The fracture surface has a large number of dimples and a small number of cleavage planes, the fracture mode of the alloy is a mixed mode of ductile and brittle fractures,

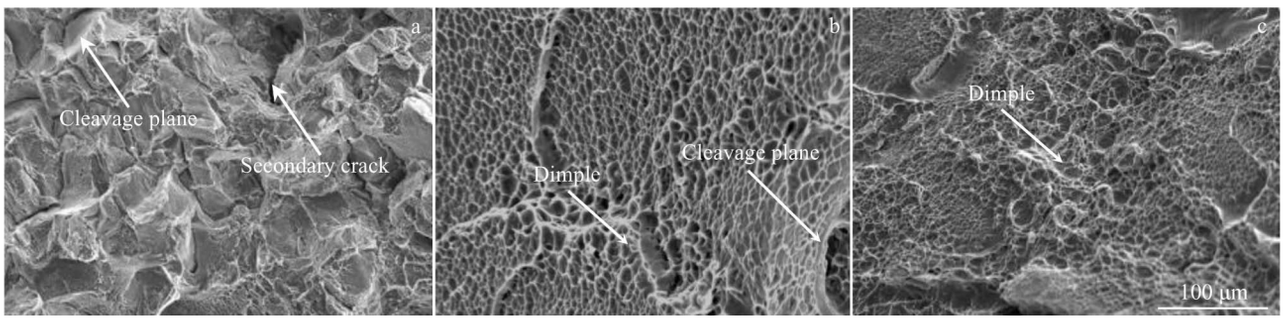

Fig.5 Fracture surfaces of Ti-5.5Cr-5Al-4Mo-3Nb-2Zr alloy after different heat treatments: (a) SX, (b) GR, and (c) ABFCA

and ductile fracture is prior to brittle fracture, so the alloy has excellent ductility. The fracture morphology of the alloy after ABFCA treatment is shown in Fig. 5c. Many deep dimples are observed, indicating that the fractured surface of the sample has very good ductility. However, it can be clearly seen that compared with those after ABFCA heat treatment, the number of dimples on the fracture surface is more, the depth is deeper, and the size is larger after GR heat treatment. Therefore, the ductility of the alloy after GR heat treatment is slightly higher than that of the alloy after ABFCA heat treatment.

2.4 TEM microstructure

The microstructure of the stretched alloy was observed by TEM, and the results are shown in Fig. 6. When the alloy is aged, a large number of fine α_s phases can be observed, and a large number of dislocations are accumulated on the α_s/β interface (Fig. 6a). When the alloy is solution treated, a small number of α_p phases can be clearly observed. The β matrix exhibits a large number of dislocations, which are also observed in the α_p phase (Fig. 6b). When the alloy is ABFCA treated, there are a large number of secondary phases of different sizes in the alloy, including the α_s phase, α_p phase and α_r phase (Fig. 6c). Many substructures are found in the α_p phase, which are identified as twins by SAED analysis (Fig.6d).

After solution treatment, the alloy displays remarkable ductility because the volume fraction of the β matrix is higher than that of the secondary phase, and the dislocation can slip freely in the β matrix.

In alloys, slip usually occurs firstly, and then twin nuclei are generated by extremely high stress at the dislocation plug. Once the twin is formed, as long as the shear stress is above a certain critical value, the twins can propagate. When the alloy is treated with ABFCA, twins in the α_p phase are identified. The Ti-5.5Cr-5Al-4Mo-3Nb-2Zr alloy undergoes deformation before cracking occurs. There are many deformation mechanisms, such as slip and twins. Dislocation slip is a vital deformation mechanism in this titanium alloy, and

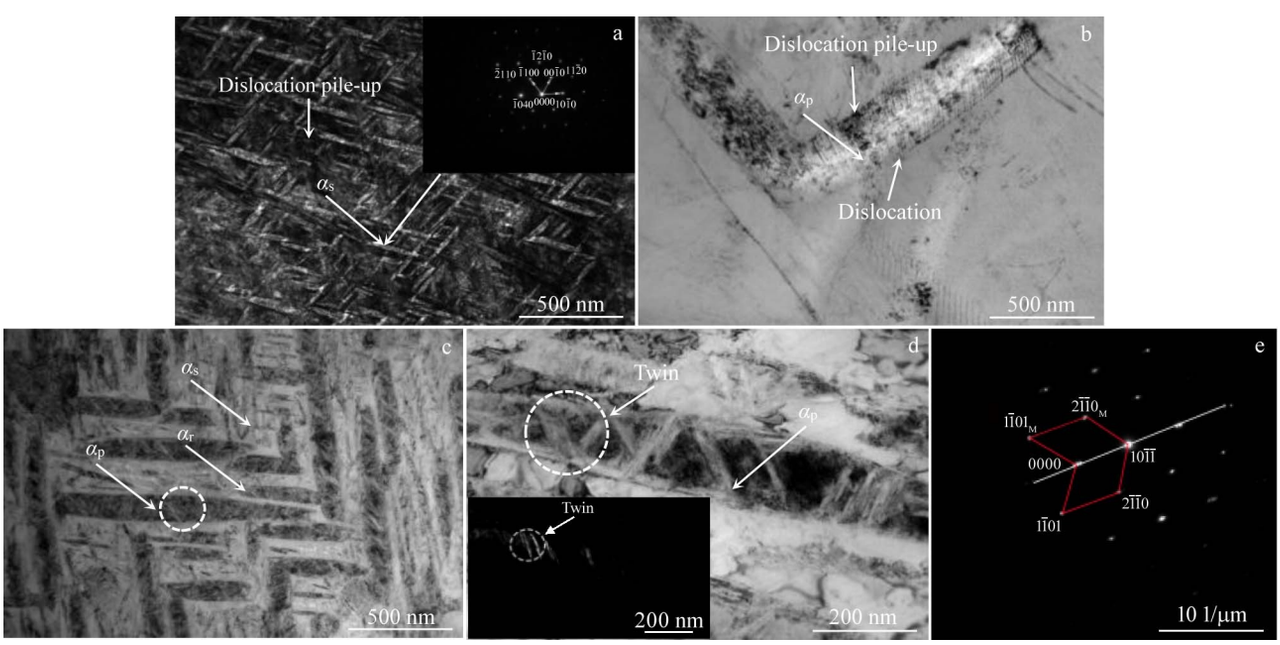

Fig.6 TEM images of deformation microstructure after different heat treatments: (a) SX (upper right inset is SAED pattern), (b) GR, and (c) ABFCA; (d) magnified image of the circle area marked in Fig.6c (lower left inset is a dark field image), (e) SAED pattern of the circle region marked in Fig.6d

deformation twin is another important deformation mechanism. Dislocation slip and deformation twins are usually coordinated processes, and twins occur when the slip process becomes difficult. In turn, twins can initiate some slip systems that are previously difficult to initiate and promote the maintenance of dislocation slip[27]. Certain dislocations that are prone to slip are transferred into well-oriented α precipitated phases and form dislocation tangles. The α_p phase is deformed by twins at higher local stresses due to dislocation stacking at the α/β interface, and the twin mechanism occurs due to the accumulation of stratification faults in a continuous plane and extension over the entire width of the grain or phase. The α_p phases with large α/β interfaces are more susceptible to slip transferring, and can withstand more deformation, resulting in adaptation to greater strains and high ductility. The generation of twins changes the orientation of some crystals so the original unfavorable part of the alloy in the deformation process smoothly occurs in slip deformation. Thus, the stress concentration can be relaxed and the amount of ductile deformation before fracture is increased[28].

2.4.1 Effect of α_p phase on tensile properties of alloy

The dislocations in the α_p phase can slip and accumulate at the α_p/β interface (Fig. 6b). Fig. 7 shows a schematic diagram of dislocation slip in the α_p phase. The term $N\tau b$ denotes the local stress, where τ represents the applied stress and b stands for the value of Burgers vector. The dislocations nestled within the leading edge of the interface will experience a stress field τ^* and consequently generate an equal and opposite force $\tau^* b$. At equilibrium, the equation can be expressed as follows[29].

$$N\tau b\cos\theta = \tau^* b \tag{4}$$

The number of dislocations (N) can be calculated, as follows.

$$N = (1-\upsilon)\pi\lambda_\alpha(1/2Gb) \tag{5}$$

where λ_α is the width of the α_p phase, υ refers to Poisson's ratio and G refers to the shear modulus. The critical stress τ_2 of dislocation sliding is calculated as follows.

$$\tau_2 = \left[\frac{2Gb\tau^*}{(1-\upsilon)\pi\cos\theta}\right]^{1/2}\lambda_\alpha^{-1/2} = k\lambda_\alpha^{-1/2} \tag{6}$$

where k is a material constant.

Eq. (6) illustrates that τ_2 is proportional to the power of $-1/2$ of λ_α. The strengthening effect increases as the width of the α_p phase decreases. The same formula can be applied to the length of the phase. A smaller α phase is obtained after heat treatment, and a higher strength of the alloy is obtained. The size of the α_s phase is much smaller than that of the α_p phase, so the strengthening effect is more obvious.

2.4.2 Effect of α_s phase on tensile properties of alloy

As shown in Fig. 6a, dislocations in the β matrix can slip freely and accumulate at the interface when the slip is hindered by the α_s/β interfaces. Meanwhile, the diagram of dislocation slip in the β matrix is shown in Fig. 8. τ_3 represents the critical stress at which the dislocation propagates through the α_s/β interface, which can be calculated by Eq.(7).

$$\tau_3 = \left[\frac{2G_1 b_1\tau_1^*}{(1-\upsilon_1)\pi}\right]^{\frac{1}{2}} S_\alpha^{-\frac{1}{2}} = k_2 S_\alpha^{-\frac{1}{2}} \tag{7}$$

where k_2 is a material constant and S_α is the average spacing of the α_s phase.

The strengthening effect of the α_s phase decreases as the average spacing α_s phase increases.

2.4.3 Effect of α_r phase on tensile properties of alloy

As shown in Fig. 6c, Zhu et al[30] have also observed the similar phenomenon in the process of studying metastable β titanium alloys. In the deformation process, the α_s phase is not easily deformed, and the β matrix is easily deformed, so the strain incompatibility effect will occur between the α_s and the β matrix, and the poor ductility of the alloy will be obtained. This phenomenon also occurs between the α_p phase and β matrix, but the deformation ability of the α_p phase is higher than that of the α_s phase, and poor strength of the alloy is obtained. However, multi-scale α phase causes more homogeneous strain distribution, and the α_r phase is a medium-sized precipitated phase with a moderate deformation ability between that of the α_p phase and α_s phase. Plastic deformation begins at the α_p phase, and with increasing the stress, a large number of dislocations are accumulated on the α_p/β interface. When the stress reaches a certain value, the plastic deformation of the α_p phase will no longer occur, the plastic deformation of the α_r phase will be activated, and the α_s phase is the last phase to undergo deformation (Fig. 9). This process makes the alloy have very uniform strain distribution in the tensile process, and excellent strength and ductility of the alloy are obtained.

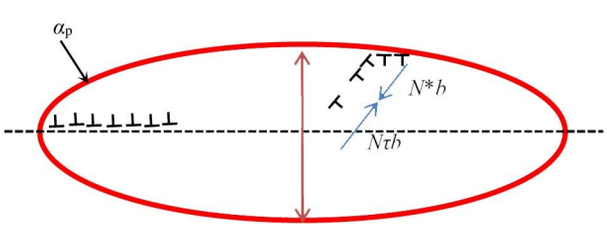

Fig.7 Schematic diagram of dislocation slip in the α_p phase after GR treatment

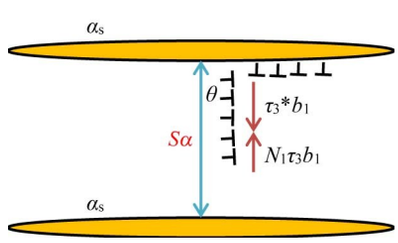

Fig.8 Schematic diagram of dislocation slip in the β matrix after SX treatment

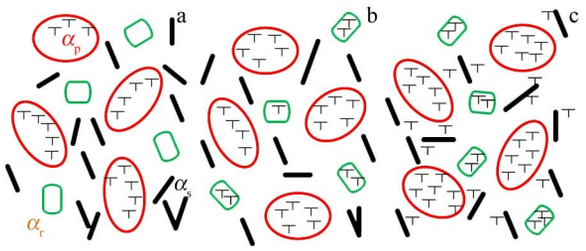

Fig.9 Schematic diagrams of plastic deformation of multi-scale α phase after ABFCA treatment: (a) accumulation of dislocations in the α_p phase, (b) accumulation of dislocations in the α_p and α_r phases, and (c) compatible plastic deformation

3 Conclusions

1) A novel metastable β titanium alloy Ti-5.5Cr-5Al-4Mo-3Nb-2Zr is designed by molybdenum equivalent and d-electron theory, and a new heat treatment process (ABFCA) is used to introduce α phases of different sizes into the matrix.

2) Compared with the aging treatment and solution treatment, the alloy obtained by the ABFCA heat treatment shows an obvious balance between strength (UTS=1125.4 MPa) and ductility (EL=18.3%).

3) An acceptable strength is obtained by ABFCA heat treatment, and the α/β interface that prevents dislocation slip is one of the important reasons for the strength improvement of the alloy. The alloy has excellent ductility because the α_r phase solves the problem of strain incompatibility; at the same time, the twins in the α_p phase play a crucial role in improving the ductility of the alloy.

References

1 Huang Chaowen, Zhao Yongqing, Xin Shewei *et al. Rare Metal Materials and Engineering*[J], 2017, 46(S1): 67 (in Chinese)

2 Abbasi S M, Momeni A, Lin Y C. *Materials Science and Engineering A*[J], 2016, 665: 154

3 Zhang Haoyu, Li Xiaohui, Lin Li *et al. Rare Metal Materials and Engineering*[J], 2019, 48(12): 3812

4 Pralhad Pesode, Shivprakash Barve. *Journal of Engineering and Applied Science*[J], 2023, 70: 128

5 Huang Chaowen, Ge Peng, Zhao Yongqing *et al. Rare Metal Materials and Engineering*[J], 2016, 45(1): 254 (in Chinese)

6 Santhosh R, Geetha M, Saxena V K *et al. Journal of Alloys and Compounds*[J], 2014, 605: 222

7 Lu Jinwen, Ge Peng, Zhao Yongqing *et al. Rare Metal Materials and Engineering*[J], 2014, 43(6): 1441 (in Chinese)

8 Gu Kaixuan, Zhao Bing, Weng Zeju *et al. Materials Science and Engineering A*[J], 2018, 723(18): 157

9 Ding Chao, Shi Qi, Liu Xin *et al. Materials Science and Engineering A*[J], 2019, 748(4): 434

10 Zhang Haoyu, Li Xiaohui, Lin Li *et al. Rare Metal Materials and Engineering*[J], 2019, 48(12): 3812

11 Sun Zhichao, Li Xuanshuang, Wu Huili *et al. Materials Characterization*[J], 2016, 118: 167

12 Zhao Yongqing, Zeng Weidong, Lin Cheng. *Materials China*[J], 2009, 28(6): 51 (in Chinese)

13 Zhu Zhishou, Wang Xinnan, Gu Wei *et al*. *Materials China*[J], 2009, 28(2): 51 (in Chinese)

14 Qin Haixu, Geng Naitao, Yang Liu *et al*. *Titanium Industry Progress*[J], 2023, 40(3): 6 (in Chinese)

15 Du Zhaoxin, Liu Guolong, Cui Xiaoming *et al. Rare Metal Materials and Engineering*[J], 2019, 48(6): 1904 (in Chinese)

16 Dong Ruifeng, Li Jinshan, Kou Hongchao *et al. Journal of Materials Science & Technology*[J], 2019, 35(1): 48

17 Liang Huang, Chang Minli, Cheng Linli *et al*. *Transactions of Nonferrous Metals Society of China*[J], 2022, 32: 3835

18 Chen Fuwen, Xu Guanglong, Zhou Kechao *et al*. *Journal of Materials Science*[J], 2020, 55: 3073

19 Song Bo, Yu Chen, Xiao Wenlong *et al. Materials Science and Engineering A*[J], 2020, 793: 139886

20 Wang Ke, Zhao Yongqing, Jia Weiju *et al. Rare Metal Materials and Engineering*[J], 2021, 50(2): 552 (in Chinese)

21 Song Ping, Li Wenbin, Zheng Yu *et al. Journal of Alloys and Compounds*[J], 2019, 811: 151946

22 Zhang Chongle, Bao Xiangyun, Zhang Jinyu *et al. Rare Metal Materials and Engineering*[J], 2021, 50(2): 717 (in Chinese)

23 Clodualdo Aranas, Anes Foul, Baoqi Guo *et al. Scripta Materialia*[J], 2017, 133: 83

24 Song Bo, Xiao Wenlong, Ma Chaoli *et al. Materials Characterization*[J], 2019, 148: 224

25 Lan Yongting, Mian Jia. *Materials Today Communications*[J], 2023, 38: 107645

26 Takeshi Nagase, Takao Hori, Mitsuharu Todai *et al. Materials & Design*[J], 2019, 173: 107771

27 Lee Hyeon Jin, Kim Jae Hyuk, Park Chan Hee *et al. Acta Materialia*[J], 2023, 248: 118763

28 Mansur Ahmed, Elena V Pereloma *et al. Journal of Alloys and Compounds*[J], 2022, 910: 164794

29 Zhu Wenguang, Lei Jia, Zhang Zhixin *et al. Materials Science and Engineering A*[J], 2019, 762: 138086

30 Zhu Wenguang, Lei Jia, Tan Changshegn *et al. Materials & Design*[J], 2019, 168: 107640

不同尺寸的α相对亚稳β钛合金Ti-5.5Cr-5Al-4Mo-3Nb-2Zr拉伸性能的影响

劳振宏[1]，张浩宇[1]，王圣元[1]，程　军[2]，谭　兵[1]，周　舸[1]，张思倩[1]，陈立佳[1]

(1. 沈阳工业大学 材料科学与工程学院，辽宁 沈阳 110870)

(2. 西北有色金属研究院 陕西省医用金属材料重点实验室，陕西 西安 710016)

摘　要：为了研究新型亚稳β钛合金Ti-5.5Cr-5Al-4Mo-3Nb-2Zr的微观组织与拉伸性能之间的关系，设计了一种可以在β基体中析出不同尺寸α相的ABFCA热处理工艺（在α+β相区进行固溶处理，然后随炉冷却，最后进行时效处理）。这种热处理工艺获得的微观组织由初生α相（α_p）、亚微米级棒状α相（α_r）和次生α相（α_s）组成。结果表明，具有多尺寸α相的合金具有较高的强度和极好的塑性。当合金的极限抗拉伸强度为1125.4 MPa时，合金的断后伸长率可以达到18.3%。建立了合金强度与α相之间的关系，即合金的强度与α相的宽度以及平均间距的–1/2次幂成线性关系，尺寸和相间距较小的α_s相通过对位错滑移的阻碍作用使合金的强度大大提高。透射电子显微镜观察表明，在α/β界面上存在大量的位错塞积，而且在拉伸变形之后的α_p相内发现了大量的形变孪晶。当位错滑移受到阻碍时，在应力集中处萌发孪晶，而孪晶又可以启动一些难以滑移的位错，同时塑性应变在α_p、α_r、α_s相和β基体中均匀分布，使得合金的塑性有较大提升。

关键词：亚稳β钛合金；α相；热处理工艺；拉伸性能

作者简介：劳振宏，男，1995年生，硕士，沈阳工业大学材料科学与工程学院，辽宁 沈阳 110870，E-mail：13596265975@163.com